Computational experiments on three-dimensional molecular diffusion in porous media

Vladimir J. Alarcon*, William Kingery**, Jianping Zhu***

* Geo-Resources Institute, ERC, Mississippi State University, Mississippi State, Box 9627, MS 39762.
Phone: +1-662-325-7704; Fax: +1-662-325-7692; E-mail: alarcon@gri.msstate.edu
** Plant and Soil Sciences Department, Mississippi State University, Mississippi State, MS 39762, USA
*** Department of Theoretical and Applied Mathematics, University of Akron, Akron, OH 44325, USA

ABSTRACT

Estimations of apparent diffusion coefficients usually consist of curve-fitting the output of 1-D models to experimental laboratory-measured data from porous aggregates shaped in different forms. In this research, a computational exploration is presented on the alternative use of three-dimensional models for the same purpose. The outputs of the 3-D models were compared to results generated by one-dimensional formulations. The comparison showed that there are significant discrepancies in the concentration values output by the models. Percent differences ranging from 30 to 90% were calculated. Those different estimations suggest that different values of the apparent diffusion coefficient may be obtained if the three-dimensional solution of the diffusion equation would be used to match experimental results.

Keywords: computational simulation, porous media, molecular diffusion

1 INTRODUCTION

The transport of contaminants within porous media occurs through pathways such as passive mass flow (dissolved solute moves with the moving water), liquid diffusion (solutes move within the solution by intermolecular interactions), and vapor diffusion (diffusion of solute vapor molecules in the pore air spaces).

Conceptual models of liquid transport of solutes in porous media (such as soil) oftentimes partition the porous media matrix in regions where: a) mobile phase where the solution flows fast and is governed by advective-dispersive phenomena, and, b) non-mobile phase where no advection is present and the transport of the solute is pre-dominantly due to molecular diffusion.

The mathematical theory of diffusion of a substance in isotropic substances [3] is described by:

$$\frac{\partial C}{\partial t} = D\left(\frac{\partial^2 C}{\partial x^2} + \frac{\partial^2 C}{\partial y^2} + \frac{\partial^2 C}{\partial z^2} \right). \qquad (1)$$

In Equation (1), C is the concentration of diffusing substance and D the diffusion coefficient in free solution. To account for the retardation caused by the partition of the solute and the tortuosity of the diffusion path, an effective (or apparent) diffusion coefficient (D_e) is used for estimating diffusion in porous media [1]: $D_e = D\ \tau$, where τ is the tortuosity factor ($0 < \tau < 1$). Tortuosity is usually defined as the ratio of the mean path length of a dissolved species to the straight-line distance of the overall path [6].

Several experimental attempts have been done to measure or estimate key diffusion parameters (such as diffusion coefficients) using disturbed and undisturbed soil cores. All of these attempts rely on the use of a simple one-dimensional mathematical model of the diffusion process that is curve-fitted against experimental measurements to indirectly obtain the desired value. [7], [8], [9] and [10], conducted diffusion experiments under several different soil water contents using either soil columns or half-cells experimental set ups. Then, measured concentrations were compared to the output of the one-dimensional mathematical model presented in [5]:

$$\frac{\partial C}{\partial t} = D_e \frac{\partial^2 C}{\partial z^2} + k\ C, \qquad (2)$$

where k is a retention coefficient. Apparent diffusion coefficients were obtained from this comparison.

[11] presented a method for estimating diffusion coefficients in low-permeability porous media (orange silty clay loam). Soil columns were set up with an annular region of repacked aquitard material and a central core of medium-grained quartz sand. The solute was transported through the central core by convection and hydrodynamic dispersion and through the annulus by radial diffusion. The effective diffusion coefficient in the aquitard material was obtained by fitting concentration measurements to the numerical output of a Crank-Nicholson solution of the radial diffusion equation in a cylinder or ring:

$$\frac{\partial C}{\partial t} = \frac{D_e}{r} + \frac{\partial}{\partial r}\left(r \frac{\partial C}{\partial r} \right), \qquad (3)$$

where r is the radius of the cylinder.

[2] assessed the influence of concentration gradients on solute transport in spherical aggregates using semi-spherical expanded clay pebbles. They estimated the intra-

aggregate diffusion coefficient by saturating individual spheres with a KBr solution. Then, they fitted the analytical solution to the radial diffusion equation for a sphere using the diffusion coefficient as the fitting parameter (r is the sphere's radius):

$$\frac{\partial C}{\partial t} = D_e\left(\frac{2}{r}\frac{\partial C}{\partial r} + \frac{\partial^2 C}{\partial r^2} \right). \quad (4)$$

In this research, a three-dimensional computational model of several different porous aggregates is presented. The modeled porous media consists of particles that are arranged stochastically to approximate the actual network present inside typical soil environments. Solute diffusion into the porous media is assumed to be governed by the 3-D formulation of Fick's Law [4]. The questions that this paper intends to answer are: would the use of a three-dimensional mathematical model provide different estimations of the diffusion coefficient? If yes, to what extent are the estimations affected?

2 METHODS

To answer the questions formulated above, three modeling approaches were used. The computational experiments were set up to simulate approximately the actual laboratory experiments summarized in Section 1.

A) Several three-dimensional shapes of porous aggregates were simulated computationally. A uniform structured raster 3-D grid was used where cubical grains were randomly located taking, as a whole, a cylindrical, spherical or annular aggregate shape. In those aggregates, the tortuous 3-D paths (through which the solute diffuses) are known by the positions of the cells that are not occupied by soil grains. A 3-D version of Fick's second law (Equation 1) is solved in those free cells. It is assumed that the diffusion coefficient is known and that its value corresponds to a free-solution diffusion coefficient.

B) Values of tortuosity were calculated for each of the 3-D aggregates. The free-solution diffusion coefficient was subsequently corrected with those tortuosity values. Those effective diffusion coefficients are then introduced into the corresponding 3-D mathematical model in which grain cells are absent (i.e., Equation (1 is numerically solved without considering grain cells).

C) Effective diffusion coefficients were introduced into 1-D models represented by Equations (2) to (4).

Finally, the solute concentration results output by the three approaches are compared and analyzed.

2.1 Numerical formulation

The liquid solution in which the aggregate is submerged is assumed to be homogeneous. External Dirichlet boundary conditions are set up around, at the center or at the top of the aggregate (depending on the case), i.e., grid cells have a constant and known concentration through time: $C(t) = C_0$, $t > 0$ at the boundaries.

For the cylindrical aggregate, a constant concentration source was maintained at the top flat side. Lateral sides were maintained at zero concentration (non-diffusive surrounding wall). For the ring and sphere simulations the porous aggregates were considered to be submerged in a homogeneous solution of known and constant concentration. For all simulations, the nominal concentration value of C_0=5 was used. In all numerical experiments, grains are assumed not to adsorb or desorb and the cells representing those grains are forced to have concentration values equal to zero at all times. Cells through which the liquid solution is free to diffuse have, initially, null concentration.

2.2 Finite difference scheme (3-D model)

The backward-time-central-space algorithm is used for it provides unconditional stability in the numerical solution. With this scheme Equation (1) becomes:

$$(1+6\lambda)C_{jlm}^{n+1} - \lambda\, C_{j+1lm}^{n+1} - \lambda\, C_{j-1lm}^{n+1} - \lambda\, C_{jl+1m}^{n+1} - \lambda\, C_{jl-1m}^{n+1} - \lambda\, C_{jlm+1}^{n+1} - \lambda\, C_{jlm-1}^{n+1} = C_{jlm}^{n}, \quad (5)$$

where $\lambda = D\frac{\Delta t}{(\Delta x)^2}$, and $\Delta x = \Delta y = \Delta z$

This is a system of equations of the type: **A c = b**, where **A** is a seven diagonal sparse matrix of size $(N\text{-}2)^3$, N the number of cells in any of j, l or m directions. The vector **c**, of size $(N\text{-}2)^3$, is composed by the C_{jlm}^{n+1} unknown concentrations at time step $n+1$. **b is** a vector of $(N\text{-}2)^3$ known values composed of the concentration values at time step n plus the known concentration values provided by the external and internal boundary conditions. The internal boundary conditions are imposed by the cells that correspond to the grains and are assumed to have null concentration at all times.

2.3 Finite difference schemes for (1-D model)

Cylinder Case: Without considering retention mechanisms) the finite-difference version of Equation (2) is:

$$(1+2\lambda)C_j^{n+1} - \lambda\, C_{j+1}^{n+1} - \lambda\, C_{j-1}^{n+1} - = C_j^{n}, \quad (6)$$

where $\lambda = D_e\frac{\Delta t}{(\Delta z)^2}$ and De = $D\,\tau$.

Ring case (radial diffusion): Using BTCS, with radius= r_0, and with $\lambda = D_e\frac{\Delta t}{(\Delta r)^2}$ the following system of

equations is generated for Equation (3):

$$C_j^n + \frac{D_e \Delta t}{r_0 + j\Delta r} = \left(1 + \frac{2\lambda}{r_0 + j\Delta r}\right) C_j^{n+1} - \frac{\lambda}{r_0 + j\Delta r} C_{j+1}^{n+1} - \frac{\lambda}{r_0 + j\Delta r} C_{j-1}^{n+1}. \quad (7)$$

In Equations (6) and (7): n = 1,2,3,4…N, correspond to time steps, j = 1,2,3,4…M represent the spatial steps along the radius of the cylinder or ring.

Sphere case: Using BTCS, Equation (4) is converted to:

$$C_j^n + \frac{2D_e \Delta t}{r_0 + j\Delta r} = (1 + 2\lambda) C_j^{n+1} - \lambda C_{j+1}^{n+1} - \lambda C_{j-1}^{n+1}. \quad (8)$$

Again, n = 1,2,3,4…N, correspond to time steps, j = 1,2,3,4…M represent the spatial steps along the radius of the sphere.

3 RESULTS AND DISCUSSION

All results shown in this research correspond to a three-dimensional uniform structured grid of 17×17×17 cells. The concentration at the external boundaries was constantly kept at a nominal value of 5.0 [$M.L^{-3}$]. For all cases, D = 1.024 [$L^2.T^{-1}$], $\Delta x = \Delta y = \Delta z$ = 0.1 [L], Δt =0.1 [L]. Tortuosities were calculated using the least-resistance path algorithm providing the following mean values: $\tau_{cylinder}$ =0.807 (with standard deviation σ = 0.045), τ_{ring} =0.816 (σ = 0.047), τ_{sphere} =0.834 (σ = 0.048). Effective diffusion coefficients are calculated using $D_e = D^*\tau$, resulting in D_e = 0.826 for cylinder, D_e = 0.836 for ring, and D_e = 0.854 for sphere.

To compare the results of the two 3-D conceptual models and the 1-D models, concentration values were averaged (for the 3-D models) at the corresponding horizontal plane.

For the cylinder case (Figure 1), the upper-right figure shows results for which the algorithm described by Equation (5) was applied without considering null diffusion at the soil grain cells. However, the diffusion coefficient was corrected due to the tortuosity present in the cylindrical aggregate (D_e=0.826). The lower-right figure in Figure 3 shows results for which the diffusion coefficient was not corrected, i.e., a free solution value is used, but soil grain cells were taken into account in the computations. Results are visualized at the tenth time step. The concentration distribution in both cases is symmetrical, and values near to 1.0 are estimated around the center of the aggregate at middle horizontal planes. Figure 1 also shows a comparison charts for concentration at the tenth time step as calculated by the 1-D model and the 3-D models. The 1-D model is shown to estimate higher concentration values than those estimated by the two 3-D models. Percent differences in calculated concentration values for the cylindrical aggregate are shown in the upper chart of Figure 4. Percent differences between the 1-D and 3-D models are higher than 40% along most of the cylinder length.

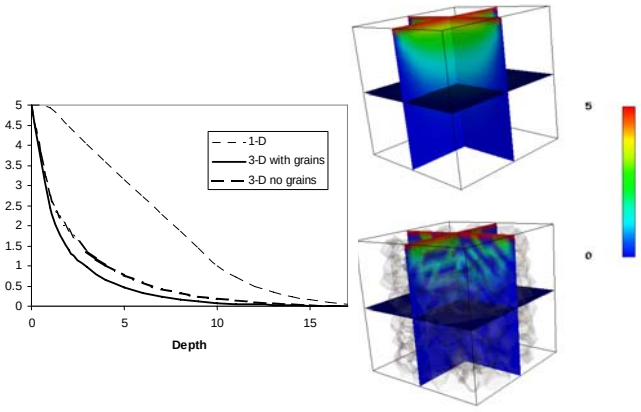

Fig. 1. Concentrations in the cylindrical aggregate at the 10th time step. Results for the simplified 3-D model with diffusion coefficient corrected by tortuosity and no soil grains (top). Results taking into account soil grains (bottom). The 1-D model estimates higher concentration values than the concentrations estimated by the 3-D models (left).

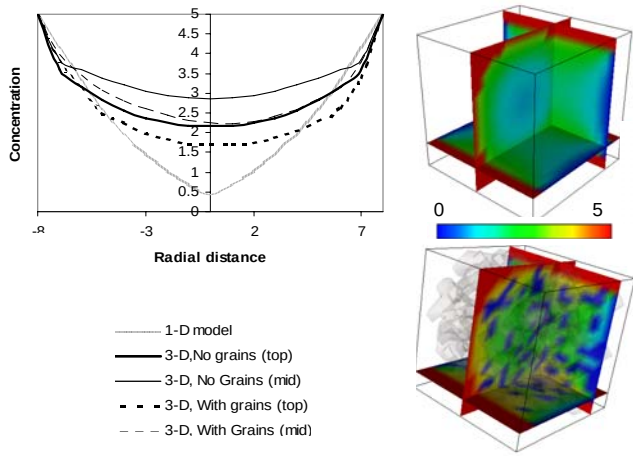

Fig. 2. Ring-shaped aggregate. Upper right figure was obtained with D_e= 0.836 (D_e= τ*D = 0.816*1.024). Lower figures for D=1.024, considering grain cells. The one-dimensional model estimates a less efficient diffusion inside the aggregate, although the diffusion seems to be more rapid at the outer ring layers at the tenth time-step.

Figure 2 shows results for the ring-shaped aggregate. Averaged results for two planes (top and middle) are also shown. At the tenth time-step the 1-D model estimates quite different values of concentration, especially near the center

of the aggregate. Percent differences of the 1-D results (with respect to 3-D results) range from 50% to 90% for regions near the center of the ring, and range from 10% to 50% the rest of the radial distances (see middle chart in Figure 4).

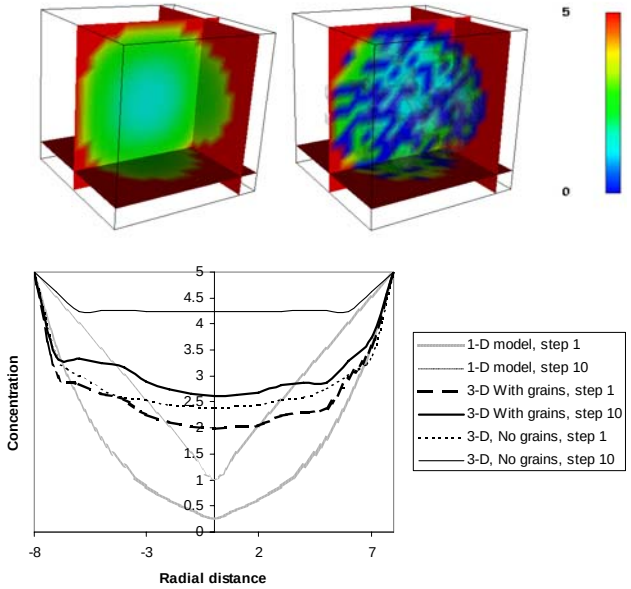

Fig. 3. Diffusion inside the spherical aggregate. As in the ring shaped aggregate, 1-D concentration estimations are shown to be smaller than those values calculated by the 3-D formulations.

For the spherical aggregate, the differences between the 1-D and 3-D models are similar as those for the cylindrical aggregate (see Figure 3). The concentration values calculated by the 1-D model at the center of the aggregate are more than 45% different from the estimations of the 3-D models (see bottom chart of Figure 4). Near the periphery of the sphere, percent differences range from 0% to 35% in absolute value. For the rest of the radial distances, percent differences are greater than 45%.

The concentration values estimated by the 3-D models for the cylinder case are shown to be smaller to those concentration estimations output by the corresponding 1-D model. For the ring and sphere cases the trend is reverse: 1-D estimations are higher than 3-D output values. This occurs because in the sphere and ring cases the grid representing the porous aggregate is surrounded by grid cells containing a constant value of non-zero concentration (C_0=5.0) through time. Therefore, molecular diffusion of the solute into the aggregate may begin at any cell at the periphery of the aggregate grid (i.e., at any cell not representing the porous material). Diffusive transport to inner free cells depends on the availability of free diffusion paths, but it is reasonable to assume that molecular diffusion into the spherical and annular aggregates is more effective than in the cylinder case because more peripheral free cells in those aggregates are exposed to the surrounding constant-concentration cells. Concentration values at positions near the center of the sphere and ring estimated with the corresponding 1-D models are lower because at those inner positions the radial diffusion models (Equations 7 and 8) only allow diffusion to occur from outer (j-1) or inner (j+1) radial positions. Three-dimensional models (Equation 5) allow diffusion from any direction (j, l, and m). Therefore, diffusion is estimated to be less effective and, correspondingly, diffusion coefficients would result smaller according to the 1-D approach.

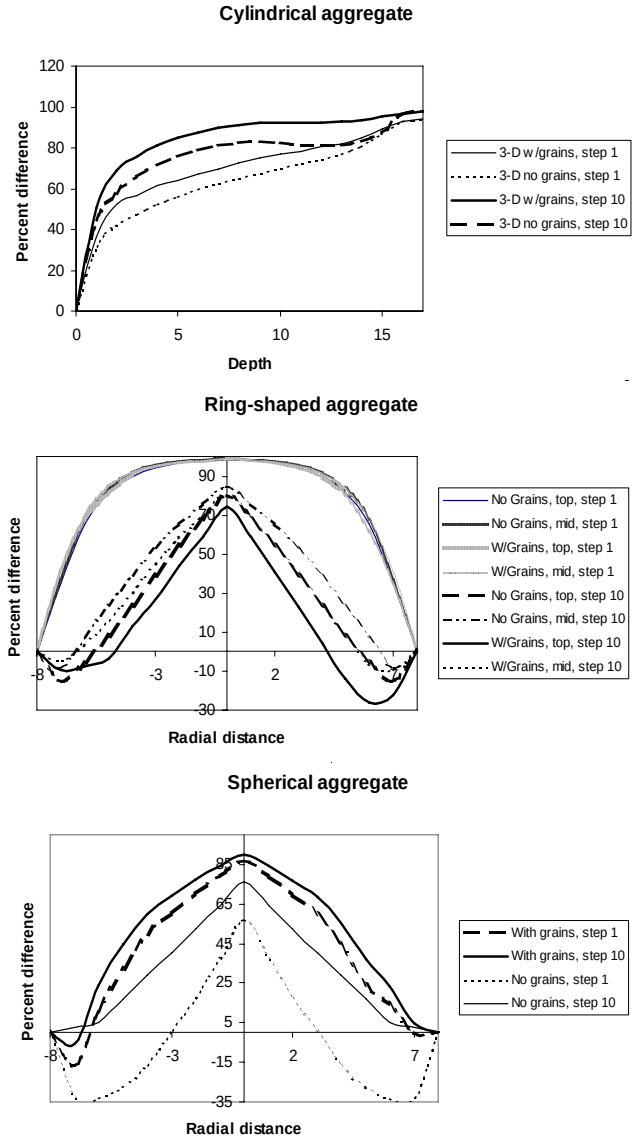

Fig. 4. Percent differences between concentration estimations of 1-D and 3-D models. Results show percent differences greater than 30% (up to 90%) in the concentration values estimated by the 1-D models with respect to the 3-D models

In the cylinder case, the aggregate is assumed to be exposed to constant concentration cells only at the top flat

side. Free cells at the bottom and the lateral outer surfaces will not have any chance of transport solute because they are not exposed to it. Therefore, three-dimensional diffusion will only occur from the top, resulting in slow transport of solute towards the bottom. Moreover, the slow transport occurring at the top portions of the aggregate will be further delayed by the imposed lateral boundary conditions that force lateral cells (external to the aggregate grid) to contain a constant concentration value of 0.0 through time (non-diffusive surrounding walls). These boundaries (that mimic sealed impermeable walls from experiments) produce a concentration dilution effect in free cells near them, resulting in a less effective three-dimensional diffusion. In the corresponding 1-D model (Equation 6) at any given cell *j*, the concentration value C_j at time $n+1$ is a linear combination of concentrations at *j*, $j+1$ and $j-1$ cells, at time-steps n and $n+1$ respectively. Therefore, as long as one of those cells contains a non-zero concentration value, cell *j* at time $n+1$ will have a non-zero value. This produces a faster transport towards the bottom of the cylinder because there is no additional concentration dilution (as that occurring in the 3-D models) since lateral boundary conditions are not necessary in the 1-D formulation.

The considerations above lead to conclude that, for the cylinder case, diffusion coefficients estimated using the 1-D model would be bigger than those diffusion coefficient values that a 3-D approach would give.

4 CONCLUSIONS

The comparison of averaged concentration values output from the 3-D models to the 1-D models results showed that there are significant discrepancies in the concentration values output by the models. Overall, all simulations show that there are percent differences greater than 30% (up to 90%) in the concentration values estimated by the 1-D models with respect to the 3-D models, along most of the depths or radial distances.

Those different estimations suggest that different values of the apparent diffusion coefficient may be obtained if the three-dimensional solution of the diffusion equation would be used to match experimental results. Further research using higher-resolution grids is necessary to test this hypothesis.

REFERENCES

[1] Clark, M. M., 1996. Transport modeling for environmental engineers and scientists. John Wiley and Sons, New York.

[2] Cote, C. M., Bristow, K. L. and Ross, P. J., 2000. Quantifying the influence of intra-aggregate concentration gradients on solute transport. Soil Science Society of America Journal, 63, 759-767.

[3] Crank, J., 1975. The mathematics of diffusion. Clarendon Press, Oxford.

[4] Dhawan, S., Erickson, L. E. and Fan, L. T., 1993. Model development and simulation of bio-remediation in soil beds with aggregates. Ground Water, 31, (2), 271-284.

[7] Moldrup, P., Kruse, C. W., Yamaguchi, T. and Rolston, D. E., 1996. Modeling diffusion and reaction in soils: I. A diffusion and reaction corrected finite difference calculation scheme. Soil Science, 161(6), 347-365.

[6] Oelkers , E. H., 1996. Physical and chemical properties of rocks and fluids for chemical mass transport calculations. In: Lichtner, P. C., Steefel, C. I. and Oelkers, E. H. (Eds.), Reactive Transport in Porous Media. Mineralogical Society of America, Reviews in Mineralogy, 34, pp 131-191.

[7] Olesen, T., Moldrup, P., Yamaguchi, T., and Rolston, D. E., 2001. Constant slope impedance factor model for predicting the solute diffusion coefficient in saturated soil. Soil Science, 166(2), 89-96.

[8] Olesen, T., Moldrup, P., Kruse, C. W., Nissen, H. H., and Rolston, D. E., 2000. Modified half-cell method for measuring the solute diffusion coefficient in undisturbed, unsaturated soil. Soil Science, 165(11), 835-840.

[9] Olesen, T., Moldrup, P., and Gamst, J., 1996a. Solute diffusion and adsorption in six soils along a soil texture gradient. Soil Science Society of America Journal, 63, 519-524.

[10] Olesen, T., Moldrup, P., Henriksen, K. and Petersen, L. W., 1996b . Modeling diffusion and reaction in soils: IV New models for predicting ion diffusivity. Soil Science, 161(10), 633-645.

[11] Young, D. F. and Ball, W. P., 1998. Estimating diffusion coefficients in low permeability porous media using a macropore column. Environmental Science and Technology, 32, 2578-2584.